ELSEVIER

Journal of Nuclear Materials 299 (2001) 250–259

journal of nuclear materials

www.elsevier.com/locate/jnucmat

Activation energy of UO_2 and UO_{2+x} sintering

Ph. Dehaudt *, L. Bourgeois, H. Chevrel

Département d'Etudes des Combustibles, Commissariat à l'Energie Atomique, CEA/Grenoble 17, rue des martyrs 38054, Grenoble cedex 9, France

Received 2 May 2001; accepted 25 July 2001

Abstract

Two methods were used to determine, in non-isothermal conditions, the sintering activation energy of UO_2 and UO_{2+x} oxides, namely the temperature increment method and the constant heating rate method. The second method is easily applied to determine activation energy with a very small standard deviation, and to check that a single process is involved during densification. This study confirmed that activation energy is significantly reduced for O/U ratios between 2.01 and 2.17 in comparison with O/U = 2.00. In contrast, it is high when there is a high proportion of U_4O_9 during sintering. Special attention is being paid to the influence of oxygen concentration preparation method on sintering activation energy kinetics. © 2001 Elsevier Science B.V. All rights reserved.

Résumé

Deux méthodes ont été mises en oeuvre pour déterminer, en condition non isotherme, l'énergie d'activation du frittage de UO_2 et UO_{2+x}, à savoir la méthode de l'incrément de température et la méthode de la vitesse de chauffage constante. La deuxième méthode est facile à appliquer pour déterminer l'énergie d'activation avec un faible écart-type et pour identifier le mécanisme qui contrôle la densification. Cette étude confirme que la valeur de l'énergie d'activation est significativement réduite pour un rapport O/U compris entre 2,01 et 2.17 par rapport à O/U = 2.00. En revanche, elle devient élevée quand la proportion d'U_4O_9 est importante au cours du frittage. Une attention particulière doit être accordée à l'influence de la méthode de préparation du titre en oxygène sur l'énergie d'activation du frittage. © 2001 Elsevier Science B.V. All rights reserved.

1. Introduction

The main theoretical relations put forward to describe the kinetics of isothermal densification, which is itself controlled by a diffusion mechanism during the first two stages of sintering, may be formulated by the general sintering equation

$$y^n = \left(\frac{\Delta l}{l_0}\right)^n = k(T)t, \tag{1}$$

where

$$k(T) = \frac{AD_0\Omega\gamma}{G^{\alpha k}}\,\frac{\exp(-Q/RT)}{T}$$

and $y = \Delta l/l_0$ is the relative shrinkage, γ the free surface energy, Ω the atomic volume, G the size of the crystallites, and k the Boltzmann's constant. D_0 is the pre-exponential term of the diffusion coefficient and Q the activation energy of the process controlling densification. The parameters n, A and α depend on the geometric shape chosen for the particles, and hence on the stage of sintering under consideration, as well as on the mechanism responsible for shrinkage. Experimental results are interpreted on the basis of models that are assumed to be strictly applicable. Consequently, the process has a number of limitations and is open to criticism by Bacmann and Cizeron [1] for example.

To avoid such difficulties, two non-isothermal methods were tested in order to determine the sintering activation energy of stoichiometric (UO_2) and hyperstoichiometric (UO_{2+x} with $x > 0$) uranium oxide. The temperature increment method, initially recommended by Dorn [2] for studying creep and extensively tested by

* Corresponding author.
E-mail address: dehaudt@cea.fr (Ph. Dehaudt).

0022-3115/01/$ - see front matter
PII: S0022-3115(01)00661-4

Bacmann et al. [1,3,4], was compared with a method involving sintering at constant heating rates that was developed by Wang and Raj [5]. These authors drew on the work of Young and Cutler [6] and Woolfrey and Bannister [7]. Unlike the work of Woolfrey and Bannister, their method has the advantage of not having to integrate the general sintering equation (1) in its differential form over a temperature domain.

With regard to densification mechanisms, it is now accepted on the basis of work carried out by Bacmann et al., Woolfrey [8] and Bannister and Buykx [9] that uranium diffusion at grain boundaries controls the first two stages of uranium dioxide sintering, regardless of the stoichiometric deviation x for the single-phase material UO_{2+x}. Knorr et al. [10] made a very thorough review of changes in the activation energy of self-diffusion and diffusion at grain boundaries as a function of the O/U ratio of the fuel, for x values between 0 and about 0.16.

The present study compares Dorn's method with that of controlled heating rate sintering. A variant of Wang and Raj's method is also proposed. This study supplements the data given in the literature, in particular for compositions that are the richest in oxygen, up to $x = 0.25$.

2. Methods adopted for determining sintering activation energy

2.1. Dorn's method

This method gives direct access to the activation energy. The isothermal shrinkage rate $v = \mathrm{d}y/\mathrm{d}t$ is first of all recorded at a temperature T_1 for a sintering time t. Then, following a temperature increment made as quickly as possible, the same recording is made at a temperature T_2, a few tens of degrees higher than T_1. The general sintering equation (1) is written in differential form

$$v = \frac{\mathrm{d}(\Delta l/l_0)}{\mathrm{d}t} = k(T)\frac{(\Delta l/l_0)^{1-n}}{n}. \tag{2}$$

Assuming that the microstructural state remains unchanged during the temperature increment, then the following equality is obtained:

$$\left(\frac{\Delta l}{l_0}\right)_{\text{end step } T_1} = \left(\frac{\Delta l}{l_0}\right)_{\text{beginning step } T_2}$$

implying the following for the shrinkage rates:

$$\frac{v_2}{v_1} = \frac{T_1}{T_2}\exp\left(\frac{-Q}{RT}\left(\frac{1}{T_2} - \frac{1}{T_1}\right)\right)$$

from which the activation energy may be deduced

$$Q = \frac{RT_1T_2}{T_2 - T_1}\ln\left(\frac{T_2v_2}{T_1v_1}\right). \tag{3}$$

As stressed by Bacmann et al., Dorn's method dispenses with:

(i) The need for a theoretical model since it is no longer necessary to draw on different theoretical equations depending on the stage of densification being studied.

(ii) The changes in grain size at the end of the second stage and during the third stage because the microstructural state remains identical during the temperature jump from which the activation energy is calculated. This may not be the case during isothermal experiments at high densification levels.

2.2. Constant heating rate experiments

2.2.1. Use of relative shrinkage

This variant of Wang and Raj's method is discussed first, because it is simpler to formulate. Here is $\Delta l/l_0$ the relative shrinkage of the sample in terms of its length, which is usually the only experimental value monitored in a dilatometric analysis. The relative shrinkage rate is thus written as follows, according to (2)

$$\frac{\mathrm{d}y}{\mathrm{d}t} = k(T)\frac{y^{1-n}}{n}.$$

Expressing $k(T)$ and assuming $f(y) = y^{1-n}/n$, this relation becomes

$$\frac{\mathrm{d}y}{\mathrm{d}t} = k_0\frac{\exp(-Q/RT)}{G^{\alpha}T}f(y). \tag{4}$$

In the case of experiments with a constant heating rate $a = \mathrm{d}T/\mathrm{d}t$, the relative shrinkage rate may be written

$$\frac{\mathrm{d}y}{\mathrm{d}t} = a\frac{\mathrm{d}y}{\mathrm{d}T}. \tag{5}$$

By substituting the expression of $\mathrm{d}y/\mathrm{d}t$ from Eq. (5) in Eq. (4) and taking the logarithms of the expressions, the following equation is obtained:

$$\ln\left(T\frac{\mathrm{d}y}{\mathrm{d}T}a\right) = -\frac{Q}{RT} + \ln k_0 + \ln G^{\alpha} + \ln f(y). \tag{6}$$

Plotting $\ln(T(\mathrm{d}y/\mathrm{d}T)a)$ as a function of $1/T$ gives a value of Q, assuming that the terms $\ln G$ and $\ln f(y)$ are constants. This is the case when values corresponding to a given relative shrinkage y are considered for different heating rates a. With the same densification level, the grain sizes are usually identical. Experimentally, the green density of the pellets is adjusted prior to each test to ensure that grain arrangement and growth conditions are identical during densification.

2.2.2. Use of relative density ρ

The pellet samples used are cylinders of diameter D and length l. It was demonstrated in the laboratory that,

under normal compaction conditions and with normal sample dimensions ($D \sim l \sim 1$ cm), axial and diametral shrinkage during sintering are homothetic. This being the case, it is possible to link the densification rate $d\rho/dt$ with the relative shrinkage rate dy/dt. Wang and Raj thus obtained a relation of the same type as the previous one

$$\ln\left(T\frac{d\rho}{dT}a\right) = -\frac{Q}{RT} + \ln k_0 + \ln G^{\alpha} + \ln f(\rho), \tag{7}$$

where $f(\rho)$ depends only on the relative density ρ. This function is more complex than $f(y)$ as it is necessary to express l, D and y as a function of ρ for a cylindrical sample. The activation energy is determined using the same method: by monitoring different heating rate a, the values of $\ln(T(d\rho/dT)a)$ are calculated at constant relative density ρ, thus allowing Q to be determined.

3. Experimental study

3.1. Preparation of samples

Various dry process powders (batch VS 14, E310 and B89) obtained by converting uranium hexafluoride gas UF_6 into UO_2 by pyrohydrolysis and reduction were used in this study, as well as a wet process powder obtained by the AUC process (batch BN6363). Their main physical chemical characteristics are indicated in Table 1. The specific surface areas are measured by a BET method and the O/U ratios of the powders or sintered samples are determined by thermogravimetric analysis of the reduction of UO_{2+x} to $UO_{2.00}$ in hydrogen.

The various deviations to the stoichiometry of the batch VS 14 powder were adjusted by mixing the initial powder with varying amounts of U_3O_8 powder prepared by the Urox process [11]. Mixing took place in a Turbula for 10 h and the pellets were then compressed at 350 MPa using a double-acting hydraulic press.

Pressures of 250–350 MPa were applied to the other batches of powder to obtain relative green densities of between 50% and 60%. The pellets were compacted with only the die being lubricated by a fine film of stearic acid dissolved beforehand in ether.

Table 1
Main physical chemical characteristics of dry-process powder batches used in the experiments (except BN6363 – of AUC type)

Batch	O/U	H_2O (%)	Specific surface area ($m^2\ g^{-1}$)
BN 6363	2.17	0.40	5.80
E 310	2.14	0.60	2.65
VS 14	2.14	0.16	2.23
B 89	2.09	0.13	4.30

3.2. Sintering heat treatment

To determine the activation energy of stoichiometric UO_2, shrinkage was monitored with a differential vertical dilatometer with a molybdenum device, developed in the laboratory. Temperature was measured with a WRe 5/26 thermocouple placed close to the samples. As far as the tests in hyperstoichiometric conditions were concerned, an Adamel-Lhomargy Di 25 differential horizontal dilatometer with an alumina device was used. The temperatures were monitored by a Pt/Pt–10%Rh thermocouple. Heating rates were between 75 and 500 K h^{-1}.

With regard to the experiments using Dorn's method, the temperature was increased by 30 K in 1 min, and then held steady for 30 min. The recording showed that the temperature during this period was stable to within ± 1 °C about 2 min after the temperature increment. According to estimates made by Bacmann and Cizeron, who used a similar furnace configuration and sample size, the pellets also reach set point temperature about 1 min after a 20 °C increment.

When the desired oxygen concentration in the powder was obtained by adding U_3O_8, the samples were heated beforehand for 10 h at 600 °C in high-purity helium in order to synthesise UO_{2+x} from U_3O_8 and UO_2 and to ensure a consistent O/U ratio for the compacted pellets. Chevrel [12] produced compacted powder pellets containing 15% and 25% of U_3O_8 that he placed in sealed tubes. After being held at 550 °C for 10 h, X-ray diffraction analysis of the compacted pellets revealed that the U_3O_8 phase had disappeared.

Heat treatment for determining the sintering activation energy of stoichiometric UO_2 was performed in a H_2 flow. The hyperstoichiometric compacted pellets were sintered in high-purity helium or argon flows. In this case, the oxygen concentrations in the sintering atmospheres were checked at the outlet by means of an oximeter. In the range of temperatures explored, the values are about 1 vpm of O_2. According to the Ellingham diagram proposed by Lindemer and Besmann [13] for the $UO_{2\pm x}$ system, this oxygen partial pressure is higher in all cases than those in equilibrium with the samples for all stoichiometric deviations. In fact, the stoichiometric deviation is not modified in any of the 'neutral' atmospheres. This was verified by thermogravimetric analysis of the samples before and after sintering for all the experiments. The exchange kinetics between these atmospheres and the compacted pellets were too slow to make any significant modification in the oxygen content of the solids during densification. The relative densities of the sintered samples were finally determined by hydrostatic weighing in ethanol.

4. Results

4.1. Constant heating rate sintering method

This method was used for samples with an O/U ratio of 2.000 then 2.09 (batch B89) and finally 2.17 (batch BN 6363). The green densities of the compacted pellets are carefully adjusted for each O/U ratio (Fig. 1) in order to compare the densification rates $d\rho/dT$ for each heating rate a at constant relative density ρ.

Polynomial fitting of the experimental points on either side of each selected relative density value ρ was carried out systematically. Fig. 2 is an example of the curves obtained after polynomial fitting to represent the experimental points of $UO_{2.09}$ pellet sintering for $\rho = 85\%$. The temperature T and derivatives dy/dT or $d\rho/dT$ in relations (6) and (7) are obtained from the fitting process. The Arrhenius plots corresponding to relation (7) for five relative density values ρ are presented in Figs. 3(a)–(c), respectively, for the $UO_{2.00}$, $UO_{2.09}$ and $UO_{2.17}$ compositions. The activation energy values for each composition are identical, regardless of the densification rate ρ adopted. A single process is involved meaning that no difference between the first and second stages appeared. However, the first calculation was performed at a relative density $\rho = 60\%$ for which the first stage would be finished. The average values obtained and the uncertainties are 429 ± 8 kJ mol^{-1} for $UO_{2.00}$, 242 ± 6 kJ mol^{-1} for $UO_{2.09}$ and 299 ± 9 kJ mol^{-1} for $UO_{2.17}$ (Table 2). Using this method with polynomial fitting reduced the relative uncertainties on activation energy values to 2–3%.

In the case of stoichiometric UO_2, the calculations were performed for five relative density values between

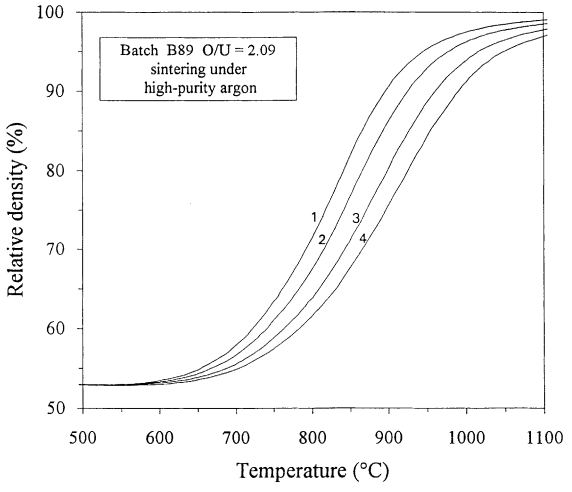

Fig. 1. Densification for constant heating rate experiments. Rates are 75, 150, 300 and 500 K h^{-1}, corresponding to plots 1–4.

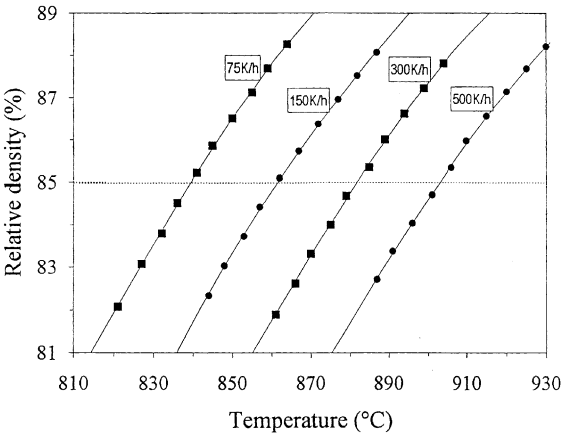

Fig. 2. Detail of densification curves according to heating rate used. The experimental points are represented by the symbols (■, ●) and the solid lines correspond to the polynomial fittings adopted. For a given relative density (here $\rho = 85\%$), the derivatives $d\rho/dT$ and the corresponding temperatures are calculated from the polynomial.

65% and 85%, corresponding to the 1150–1400 °C temperature range. In the case of the $UO_{2.09}$ and $UO_{2.17}$ compacted pellets, the relative densities, or equally the corresponding temperatures, were chosen in such a way as to remain within the UO_{2+X} single-phase domain. According to the phase diagram (Fig. 4), the U_4O_9 type phase disappears above 500 °C in the case of an O/U ratio of 2.09 and above about 750 °C for 2.17. On the basis of these data, calculations were performed for $UO_{2.09}$ at $\rho \geqslant 60\%$, i.e., at temperatures above 700 °C, irrespective of heating rate (Fig. 1). Calculations were performed for $UO_{2.17}$ at $\rho \geqslant 65\%$, i.e., at temperatures of 765, 785 and 800 °C, at heating rates of 150, 300 and 500 K h^{-1}, respectively.

Lastly, Table 3 shows that relations (6) and (7) lead to similar activation energy values. The very good agreement found means that it is possible to work directly on the relative shrinkage values recorded by the dilatometer.

4.2. Dorn's method

For stoichiometric UO_2, temperature increments were applied from 900 to 1200 °C, using batch E 310. The average value obtained in the first and second stages of sintering was 381 ± 37 kJ mol^{-1} (Table 4).

For the hyperstoichiometric compositions studied here (2.087, 2.116, 2.145 and 2.174), the temperature increments began at 900 °C in order to measure activation energy in the UO_{2+x} single-phase domain. The presence of U_4O_9 could not be avoided in the case of compositions with a higher oxygen content, unless the study started at temperatures above 1000 °C. Then, as

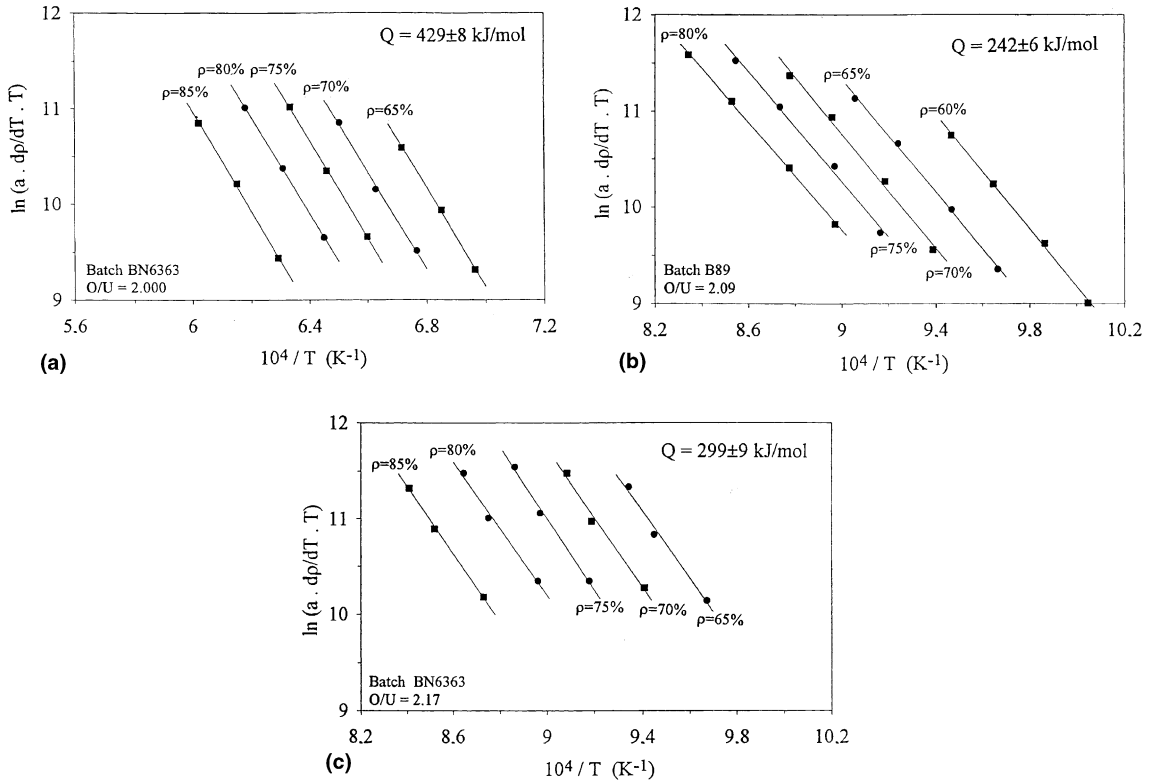

Fig. 3. (a) Plots used to determine activation energy according to relation (7) for $UO_{2.00}$. Sintering in H_2. $a = 75$, 150 and 300 K h^{-1}. (b) Plots used to determine activation energy according to relation (7) for $UO_{2.09}$. Sintering in Ar. $a = 75$, 150, 300 and 500 K h^{-1}. (c) Plots used to determine activation energy according to relation (7) for $UO_{2.17}$. Sintering in Ar. $a = 150$, 300 and 500 K h^{-1}.

Table 2
Sintering activation energy for UO_{2+x} using the constant heating rate method

Composition	Q (kJ mol^{-1})	S.D.
$UO_{2.00}$	429.1	±7.8
$UO_{2.09}$	242.4	±5.8
$UO_{2.17}$	299.0	±8.9

Chevrel et al. [15] had pointed out, samples with a high O/U ratio reached densification of about 90%, which is close to the third stage of sintering. A change in densification mechanism may occur if a fraction of the porosity becomes intergranular. Moreover, grain growth may begin. The temperature increments adopted for high O/U compacted pellets were therefore within a restricted temperature domain (Table 5). Table 5 shows the activation energy values obtained for various compositions, together with the uncertainty values which range from 8% to 10% on average, in agreement with the results obtained by Bacmann and Cizeron. The main source of uncertainty with this method comes from extrapolating the experimental points in order to obtain the shrinkage rate v_2 at the time of the temperature increment.

5. Discussion

5.1. Comparison with previous results

5.1.1. Stoichiometric uranium dioxide

Fig. 5 gives all the values adopted by Knorr et al. together with the results obtained here using Dorn's method and by constant rate sintering. It can be seen that the value obtained with Dorn's method ($Q = 381 \pm 38$ kJ mol^{-1}) is in good agreement with that proposed by Knorr et al. as being most representative of the data provided by the same method ($Q = 377$ kJ mol^{-1}) for diffusion at grain boundaries. In contrast, the constant heating rate method provides a higher energy value ($Q = 429 \pm 8$ kJ mol^{-1}), corresponding to the upper limit of the uncertainty interval on values obtained by Dorn's method. However, the constant heating rate method introduces less uncertainty on the determination of activation energy during shrinkage. This small standard deviation, which is

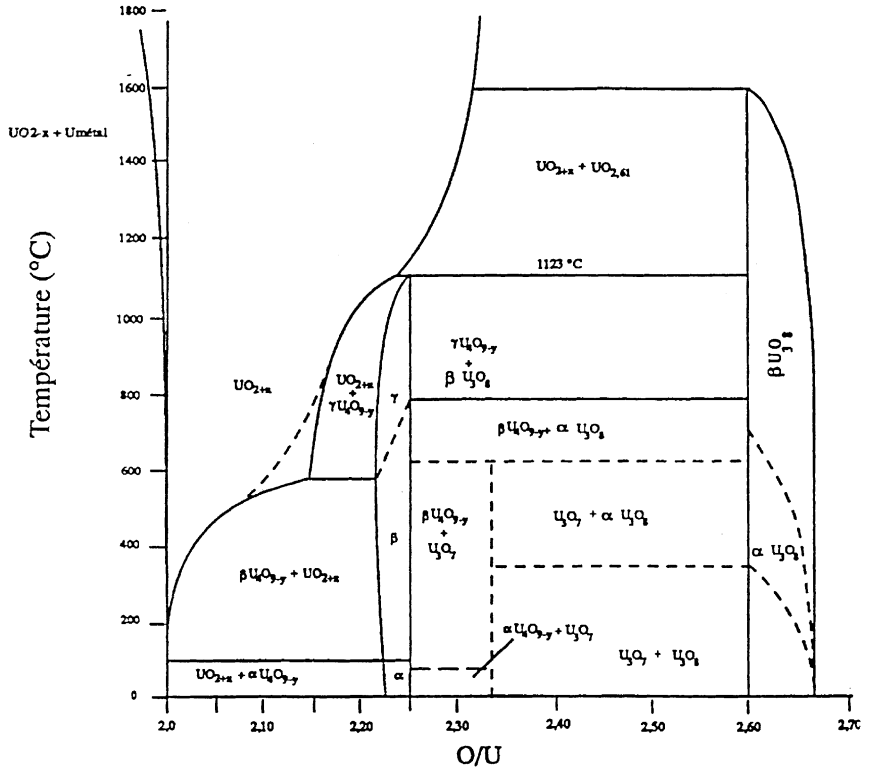

Fig. 4. Equilibrium phase diagram according to [14].

Table 3
Constant heating rate sintering method: comparison of results using relative shrinkage rate dy/dT and relative densification rate $d\rho/dT$[a]

Relative density ρ (%)	Q (kJ mol^{-1})	
	With dy/dT	With $d\rho/dT$
60	245.9	247.8
65	246.3	245.1
70	248.5	247.7
75	239.5	238.1
80	234.3	233.2
Mean (kJ mol^{-1})	242.9	242.4
S.D.	±5.2	±5.8

[a] $UO_{2.09}$ composition. Heating rates $a = 75$, 150, 300 and 500 K h^{-1}.

Table 4
Sintering activation energy for stoichiometric UO_{2+x} using Dorn's method (batch E310)

T_1 (°C)	T_2 (°C)	Q (kJ mol^{-1})
900	930	367.2
930	960	384.0
960	990	388.5
990	1020	454.3
1020	1050	408.0
1050	1080	312.9
1080	1110	342.6
1110	1140	401.0
1140	1170	371.8
1170	1200	396.5
	Average (kJ mol^{-1})	381.1
	S.D.	±37.9

revealed by parallel straight lines (Figs. 3(a)–(c)), also means that no effect on grain growth is observed in the density domain studied here.

5.1.2. Hyperstoichiometric uranium dioxide

Fig. 6 gives all the values taken into account by Knorr et al. on the basis of sintering or creep experiments and also by tracer-based diffusion coefficient measurements for deviations with respect to stoichiometry between $x = 0$ and 0.16. The diffusion activation energy at grain boundaries appears to increase from 377 kJ mol^{-1} for stoichiometric UO_2 ($x < 10^{-4}$) to a virtually constant value of 238 kJ mol^{-1} for $0.01 < x < 0.16$. The transition between the two domains occurs for a very small stoichiometric deviation, the value of which is not accurately determined because controlling

Table 5
Sintering activation energy for UO_{2+x} using Dorn's method[a]

Temperatures		Stoichiometric deviation						
T_1 (°C)	T_2 (°C)	0.087	0.116	0.145	0.174	0.197	0.223	0.258
900	930	305.6	317.3	360.4	347.4	555.0	446.5	546.9
930	960	310.5	323.4	364.8	333.9	461.2	434.5	533.9
960	990	285.3	309.8	339.5	381.6	438.2	420.3	459.3
990	1020	290.6	329.7	319.4	298.7	483.3	437.0	494.4
1020	1050	289.1	283.2	287.5	310.4	359.3	444.7	–
1050	1080	284.5	303.0	286.5	309.4	591.7	–	–
1080	1110	297.7	382.8	276.5	249.7	–	–	–
Average (kJ mol^{-1})		294.7	322.7	320.6	318.8	481.4	436.6	508.6
S.D.		±10.2	±31.1	±36.9	±41.5	±76.5	±10.4	±39.7
S.D. (%)		±3.5	±9.6	±11.5	±13	±14.6	±2.4	±7.8

[a] The basic powder corresponds to batch VS 14 (O/U = 2.08) with the stoichiometric deviation adjusted by adding U_3O_8 (5–30%).

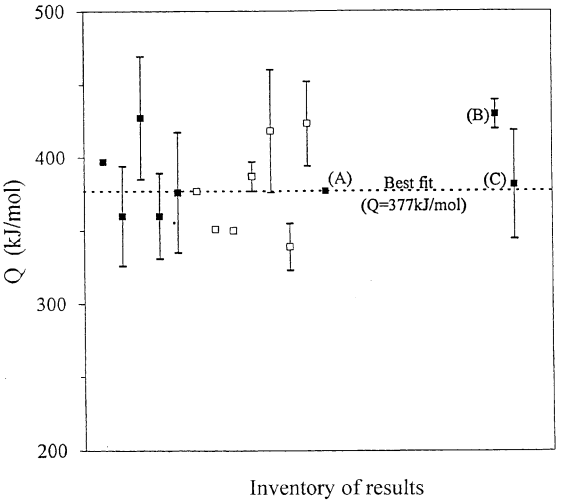

Fig. 5. Activation energy values reviewed by Knorr et al. for diffusion at grain boundaries, on the basis of creep experiments (□) and sintering (■). The solid line is the value considered to be representative: (A) proposed by Une [16]; (B) according to Fig. 3(a); (C) according to present work using Dorn's method.

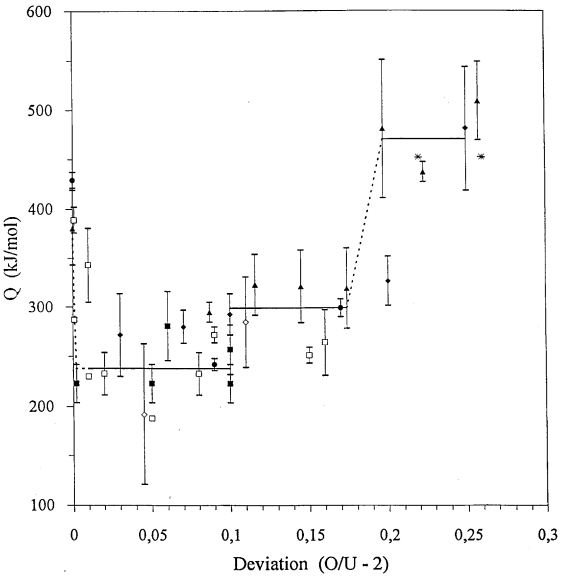

Fig. 6. Change in sintering activation energy with stoichiometric deviation x (■, □, ◇) according to Knorr et al. (Fig. 5), respectively, for sintering, creep and tracer-based diffusion coefficient measurement: (◆), according to Bacmann et al. (Dorn's method); (∗), according to Araoz; (●), according to this study (constant heating rate method); (▲), according to this study (Dorn's method).

and maintaining such small deviations is extremely difficult.

The measurements made by Bacmann et al. for $x = 0.03$, 0.07, 0.10, 0.20 and 0.25 are also shown in Fig. 6, together with the results obtained by the two methods tested in this study (Tables 2 and 5). In light of these results, the activation energy is steady up to $x \sim 0.17$. Bannister and Buykx proposed $Q = 223 \pm 19$ kJ mol^{-1} for $0.002 < x < 0.1$, Armstrong and Irvine [17] $Q = 233 \pm 21$ kJ mol^{-1} for $0.02 < x < 0.08$ and Bacmann et al. Q ~ 280 kJ mol^{-1} for $0.03 < x < 0.16$.

In the present study, Dorn's method also produces a constant activation energy value with a mean of $Q = 314 \pm 32$ kJ mol^{-1} for $0.087 < x < 0.174$ (Table 5). This value, which is significantly higher than the mean proposed by Knorr et al. is nevertheless close to the average value obtained by Bacmann et al., also using Dorn's method. For $x = 0.09$, the constant heating rate method gives $Q = 242 \pm 6$ kJ mol^{-1}, i.e., the average proposed by Knorr et al. For $x = 0.17$, the same method produces an activation energy $Q = 299 \pm 8.9$ kJ mol^{-1}, which is very close to the above mean obtained by Dorn's method (Fig. 6).

Between 0.17 and 0.20, the activation energy increases sharply by about 170 kJ mol^{-1}. Above $x = 0.20$, the activation energy appears to steady once again at 450–500 kJ mol^{-1} up to a composition of $UO_{2.25}$. Araoz [18] observed a similar variation, proposing $Q \sim 290$ kJ mol^{-1} for $0.04 < x < 0.16$ and $Q \approx 452 \pm 19$ kJ mol^{-1} for $x = 0.26$. The values obtained in the present study are also in agreement with the value published by Bacmann et al., i.e., $Q = 480 \pm 60$ kJ mol^{-1} for $x = 0.25$ (Fig. 6).

To summarise the changes occurring in activation energy as a function of stoichiometric deviation, four domains may be distinguished:

(i) For $0.01 < x < 0.1$, the value proposed by Knorr et al. ($Q = 238$ kJ mol^{-1}) would be a good compromise between the works of Bannister and Buykx, Armstrong and Irvine and the present authors (constant heating rate method).

(ii) For $0.1 < x < 0.17$, it is proposed to adopt the value of $Q = 299$ kJ mol^{-1} obtained by the constant heating rate method, which is an average between the values obtained by Bacmann et al. and those obtained here with Dorn's method.

(iii) For $0.17 < x < 0.20$, there are significant deviations, corresponding to a fast-changing domain.

(iv) For $0.20 < x < 0.25$, it is proposed to adopt $Q = 470$ kJ mol^{-1}, which is the average of the values obtained by Araoz, Bacmann et al. and the present authors for $x = 0.223$ and 0.258.

5.2. Sintering mechanism and stoichiometry

Dorn's method used for stoichiometric UO_2 provides a mean activation energy value that is in good agreement with that of U diffusion at the grain boundaries. It is now accepted that this mechanism controls the kinetics of sintering provided that pellet porosity is open and intergranular. This type of transport is predominant irrespective of pellet green density or the morphology and crystallites size of the powder used. However, when the constant heating rate method is used, the activation energy is slightly higher, with significantly less fluctuation during shrinkage. Nevertheless, this difference cannot should not be interpreted as involving another mechanism.

When $0.01 < x < 0.1$, the sintering activation energy corresponds to that of U diffusion at the UO_{2+x} grain boundaries, which is the accepted mechanism for sintering. By analogy, the activation energy for $x > 0.20$ may be considered to correspond to that of U diffusion at the U_4O_9 grain boundaries if it can be accepted that this mechanism controls its densification.

The very rapid rise in activation energy between $x = 0.17$ and 0.20 corresponds to the domain where densification occurs in the presence of two-phases UO_{2+x} and U_4O_{9-y}, according to the equilibrium phase diagram (Fig. 4). Below $x = 0.17$, the medium is single-phase UO_{2+x} and beyond $x = 0.20$ it consists mainly of U_4O_{9-y}. Consequently, it seems likely that this rapid change in activation energy is the result of progressive invasion of the grain boundaries by U_4O_{9-y}, until its presence is continuous. Indeed, when $x = 0.20$, the proportion of U_4O_{9-y} (with $y = 0.08$) is ~87 vol.%.

When $0.1 < x < 0.17$, an activation energy of $Q = 299$ kJ mol^{-1} is proposed. This is higher than the value suggested by Knorr et al. for diffusion at grain boundaries. This phenomenon may be explained by the persistence of U_4O_{9-y} during shrinkage for kinetic reasons (there is, respectively, ~43 and 73 vol.% for $x = 0.1$ and 0.17 before sintering). Knorr's compilation in this domain is based on creep measurements which are obtained in conditions such that the medium is single-phase.

Bacmann et al. suggest the presence of U_4O_{9-y} at low temperatures to explain the reduction in activation energy when the temperature rises, for $x = 0.07, 0.09$ and 0.10. The activation energy then reaches a plateau before rising again when the sample reaches the third stage of sintering, where volume diffusion becomes progressively predominant. Bacmann et al. in fact observe that the temperatures corresponding to the beginning of the activation energy values, which are of the order of 800–900 °C, are 300 °C higher than those marking the limit of the $UO_{2+x} + U_4O_{9-y}$ two-phase domain of the equilibrium diagram (Fig. 4). Bacmann et al. explain this apparent disagreement by the persistence of U_4O_{9-y}, preferably in the boundaries or their immediate vicinity.

The high activation energy values demonstrated for $x > 0.20$, which are higher than those of all the other compositions including stoichiometric UO_2, do not, however, have an adverse effect on the sintering of these compositions. Chevrel et al. noted that sintering kinetics rise continuously with increasing deviations from stoichiometry up to a composition corresponding to the U_4O_{9-y} phase. According to the review made by Knorr et al. the pre-exponential term of the intergranular diffusion coefficient D^0_{gb} increases with the stoichiometric deviation as follows:

$D^0_{gb}(UO_{2+x}) = 7.5 \times 10^{-4} x$ (m^2 s^{-1}) for $0.01 < x < 0.16$, with the activation energy being independent of x ($Q = 238$ kJ mol^{-1}).

Higher densification energies for UO_{2+x} single-phase compacted pellets with the highest oxygen contents are therefore not surprising. In contrast, the fact that samples which unquestionably contain U_4O_{9-y} should shrink more quickly suggests two possible effects:

(i) The intergranular diffusion coefficient in U_4O_{9-y} is higher than in UO_{2+x} for the temperature domain corresponding to the sintering study. This implies $D^0_{gb}(U_4O_9) \gg D^0_{gb}(UO_{2+x})$ for the pre-exponential

terms. This assumption cannot in fact be validated as no values are available for diffusion at grain boundaries in U_4O_{9-y}.

(ii) Adding U_3O_8 to adjust stoichiometric deviations does not simply enrich the oxygen content. It also helps to modify the structure of the material.

In this respect, Chevrel et al. have shown that the decomposition of U_3O_8 produces a network of fine pores enabling the samples richest in U_3O_8 to maintain a high specific surface area at equivalent densification levels. The maintenance of a high specific surface area in fact constitutes a reserve of additional energy for sintering high O/U ratio pellets. The only way of making a real comparison between the densification rates of UO_{2+x} single-phase compacted pellets (such as O/U-2 < 0.1) and two-phase compacted pellets ($UO_{2+x} + U_4O_{9-y}$, such that O/U-2 > 0.1) would be to avoid having to add U_3O_8 or else getting U_3O_8 and UO_2 to react in the powder state.

If one is not convinced of the persistence of U_4O_{9-y} when $0.1 < x < 0.17$, it should be noted that the transition of activation energy at $x \sim 0.1$ is similar to that observed for the UO_{2+x} lattice parameter at $x \sim 0.13$. As Chevrel has shown, it is indeed at this value that the nature and number of complex defects produces structural reorganisation. In the present case, this could be seen as a further demonstration of the effect of crystal arrangement on physical properties, and in particular diffusion. However, this effect should also have repercussions on the values deduced from creep reported by Knorr et al. which is not the case.

A final difficulty in validating the change in activation energy with stoichiometric deviation is the possible influence of green pellet characteristics. In contrast to the tests concerning stoichiometric UO_2, there are no systematic tests in this area for hyperstoichiometric UO_2. Bacmann et al. nevertheless showed that activation energy remains unchanged for $x = 0.10$ when the initial specific surface area of the powder changed from 3.4 to 12 $m^2\ g^{-1}$. Bannister and Buykx noted for $x < 0.10$ that activation energy was independent of relative shrinkage in the 0.5–6% range.

In compositions with a higher O/U ratio, the extent of surface diffusion or UO_3 evaporation–condensation phenomena for UO_{2+x} is not fully estimated. Chevrel et al. have nevertheless provided some micrographic proof of such activity, which is amplified as the stoichiometric deviation increases. If material is transported and redistributed by surface diffusion or evaporation–condensation, without shrinkage, then the relation between the growth of inter-particle necks and shrinkage is modified, thus distorting the general equation for sintering, as well as its extensions for non-isothermal conditions. Dilatomer measurements do not provide any information on mechanisms without shrinkage. However, in the case of $UO_{2.17}$, the straight lines in Fig. 3(a), for which the regressions are excellent over the entire heating rate range examined and for all densification levels, clearly show that a single mechanism is involved.

6. Conclusions

Two methods for determining sintering activation energy were tested and produced very similar values. The constant heating rate method proved to be very easy to use and led to very small uncertainties, of the order of 2–3%, as against 8–10% using Dorn's method.

The tests, which were concentrated mainly in the domain of the compositions richest in oxygen, revealed complex changes in activation energy as a function of the stoichiometric deviation. The persistence of U_4O_{9-y}, for kinetic reasons, as soon as $x > 0.1$, produces an activation energy that is significantly higher than that which might be expected from single-phase samples with the same stoichiometry. A U_4O_{9-y} percolation-type phenomenon is envisaged for describing the distinct increase in activation energy between $x = 0.17$ and 0.20. The activation energy of diffusion at grain boundaries in U_4O_{9-y} would be estimated at 470 kJ mol^{-1}.

References

[1] J.J. Bacmann, G. Cizeron, J. Nucl. Mater. 33 (1969) 271.
[2] J.E. Dorn, in: R. Maddin (Ed.), Creep and Recovery, American Society for Metals, Cleveland, OH, 1957, p. 255.
[3] J.J. Bacmann, G. Cizeron, J. Am. Ceram. Soc. 51 (1968) 209.
[4] J.J. Bacmann, G. Cizeron, R. Delmas, Mém. Sci. Rev. Metallurg. LXVII (2) (1970).
[5] J. Wang, R. Raj, J. Am. Ceram. Soc. 73 (1990) 1172.
[6] W.S. Young, I.B. Cutler, J. Am. Ceram. Soc. 53 (1970) 659.
[7] J.L. Woolfrey, M.J. Bannister, J. Am. Ceram. Soc. 55 (1972) 390.
[8] J.L. Woolfrey, J. Am. Ceram. Soc. 55 (1972) 383.
[9] M.J. Bannister, W.J. Buykx, J. Nucl. Mater. 64 (1977) 5714.
[10] D.B. Knorr, R.M. Cannon, R.L. Coble, Acta Metall. 37 (1989) 210.
[11] M. Pirsoul, UO_2/U_3O_8 frittable Société FBFC, Brevet d'invention français, No. 86, 08380 (10/06/1986).
[12] H. Chevrel, PhD thesis, Université de Limoges, France, No. 41, 1990.
[13] T.B. Lindemer, T.M. Besmann, J. Nucl. Mater. 130 (1985) 473.
[14] R. Keim, in: Gmelin Handbuch der Anorg Chemie: Uran System, Part C1, vol. 55, Springer, Berlin, 1977, p. 107.

[15] H. Chevrel, P. Dehaudt, B. Francois, J.F. Baumard, J. Nucl. Mater. 189 (1992) 175.
[16] K. Une, J. Nucl. Mater. 158 (1988) 210.
[17] W.M. Armstrong, W.R. Irvine, J. Nucl. Mater. 9 (1963) 121.
[18] C. Araoz, A.N.L. Report 6677, 1962, p. 388.